

## Grafted Adsorbing Polymers: Scaling Behavior and Phase Transitions

E. P. K. Currie,\* F. A. M. Leermakers, M. A. Cohen Stuart, and G. J. Fleer

*Department of Physical and Colloid Chemistry, Wageningen University, Dreijenplein 6, 6703 HB Wageningen, The Netherlands**Received April 17, 1997; Revised Manuscript Received October 21, 1998*

**ABSTRACT:** Grafted adsorbing polymers are investigated with the Scheutjens–Fleer self-consistent field model. The surface pressure of such systems is calculated numerically and semiquantitative agreement is found with experimental surface pressure isotherms of PS–PEO diblock copolymers at the air/water interface. Scaling relationships of mean-field models predict the surface pressure  $\pi$  and the height  $H$  of neutral brushes to scale as  $\pi \sim \sigma^{5/3}$  and  $H \sim \sigma^{1/3}$ , respectively, as a function of the grafting density  $\sigma$ . These scaling relationships for the surface pressure and the thickness are corroborated experimentally for long PEO chains, provided contributions to  $\pi$  due to adsorption to the air–water interface are taken into account. In the SCF model the pancake–brush transition in a good solvent is found to be continuous for all chain lengths and adsorption energies. At high adsorption energies the transition is abrupt and resembles a continuous phase transition close to a critical point, a so-called  $\lambda$ -transition.

## 1. Introduction

The physical properties of polymers end-grafted to an interface at various densities have been the subject of numerous investigations in recent years. The understanding of such systems is of importance for various natural and technical processes, for example the stabilization of colloids through (block-co)polymer adsorption,<sup>1</sup> the control of membrane architecture,<sup>2</sup> or the regulation of drug delivery through drug particles coated with biopolymers.<sup>3,4</sup> Especially systems composed of densely grafted linear polymers, so-called brushes, have attracted much attention. Theoretical studies of brushes range from relatively simple scaling models describing the properties of a brush in a good solvent<sup>5,6</sup> to sophisticated self-consistent field (SCF) analyses<sup>7–10</sup> and Monte Carlo (MC)<sup>11</sup> or molecular dynamics (MD) simulations.<sup>12</sup> The investigated properties of such polymer systems include the height and the structure of the layer as a function of grafting density and solvent conditions, the interactions of such layers with finite-sized particles,<sup>13</sup> and the collapse of the brush and domain formation in bad solvents.<sup>14–17</sup>

The conformation of linear polymers end-grafted at low density depends on the interactions between the segments, the solvent, and the surface. If the segment–surface interaction is nonattractive, a so-called mushroom structure is found. The grafted polymer has a deformed coil conformation with a radius of gyration similar to its dimensions in solution. At an increasing surface density steric interactions between polymer chains result in an anisotropic stretching of the polymers from the surface, leading to a brush conformation. de Gennes and Alexander first investigated the properties of a polymer brush using a scaling approach.<sup>5,6</sup> In a good solvent the brush conformation is determined by a balance between segment–segment excluded-volume interactions, and the entropic cost of stretching a chain. The height of the brush,  $H$ , scales as  $H \sim N\sigma^{1/3}$  where  $N$  is the length of the polymer and  $\sigma$  the number of chains per unit area. In the same model the surface

pressure scales as  $\pi \sim N\sigma^{11/6}$ . Simple analytical SCF models predict a similar scaling relationship for the brush height, that for  $\pi$  is  $\pi \sim N\sigma^{5/3}$ .<sup>17–20</sup> Under  $\Theta$  conditions the second virial coefficient is zero and the SCF scaling relationships are  $H \sim N\sigma^{1/2}$  and  $\pi \sim N\sigma^2$ , respectively.

In subsequent numerical studies the behavior of the brush thickness in a good solvent under nonadsorbing conditions has been investigated as a function of the grafting density and chain length with SCF models,<sup>7–10</sup> MC,<sup>11</sup> and MD simulations.<sup>12</sup> The results for the brush height compare favorably with the above SCF scaling relationship. A more stringent test, however, is the behavior of the surface pressure as a function of the grafting density. In two studies (SCF and MD) the surface pressure of the brush was found to deviate from the predicted  $5/3$  power law.<sup>9,12</sup> In both studies higher exponents are reported in narrow regimes with constant scaling behavior. The chains used in these studies have lengths between 25 and 200 segments. Martin and Wang found a large regime exhibiting the theoretical scaling of the surface pressure using a SCF model with chains up to 1000 segments.<sup>10</sup> They conclude that SCF scaling relationships, which take only second virial interactions into account, are indeed valid for long chains, whereas for short chains a more extended virial treatment is necessary. The good agreement between SCF scaling relationships and numerical models for the brush height of short chains is explained by the relatively weak dependence of the brush thickness on the grafting density. The numerical results therefore indicate that scaling laws for brushes should be tested experimentally using sufficiently long chains.

A number of experimental studies on brushes have examined the predicted scaling laws. In particular the power law for the brush thickness,  $H \sim N\sigma^{1/3}$ , has been investigated by several authors. One of the techniques used is measurement of the repulsive force between mica plates on which diblock copolymers with one strongly adsorbing block are deposited. Patel and Tirrell investigated polystyrene (PS) brushes in toluene with  $N$  ranging from 600 to 1500, and their results compared favorably with the predicted power law.<sup>21</sup> Poly(*tert*-butylstyrene) brushes in toluene with  $N = 30, 120$ , and

\* To whom correspondence should be addressed. Tel.: 00 31 317 482277. Fax: 00 31 317 483777. E-mail: Currie@FenK.wau.nl.

240 were investigated in a similar fashion, and a weaker scaling dependence on the degree of polymerization was found,  $H \sim N^{0.7}$ , although we remark that this exponent was found with only three data points.<sup>22</sup> In another study with PS brushes in toluene ( $N = 850$  and  $2400$ ) it was concluded that the thickness scaled more than linear with  $N$ .<sup>23</sup> As pointed out by Whitmore and Noolandi, the scaling behavior of the disjoining pressure as a function of the chain length is not equivalent to the scaling of the brush height.<sup>24</sup> The disjoining pressure between brushes is measured as a function of the distance of separation between the plates coated with the polymer. Assuming that the brush height scales as  $H \sim N$ , the disjoining pressure in this model is found to scale approximately as  $H \sim N^{1/2}$ . Their model for the disjoining pressure, however, contains four adjustable parameters. Therefore, the comparison of surface force results and scaling models for brush height is not straightforward.

The height of a brush layer of diblock copolymers adsorbed on a substrate or on an air/solvent interface can be measured directly by neutron reflectivity (NR) or neutron scattering (NS). In one study a polystyrene-poly(ethylene oxide) (PS-PEO) diblock copolymer was deposited from toluene onto quartz, on which PEO strongly adsorbs.<sup>25</sup> The layer thickness of the PS as a function of the degree of polymerization  $N$  was concluded to agree with the scaling model. As Baranowski and Whitmore pointed out, this agreement is based upon the assumption that  $H \sim \sigma^{1/3}$ .<sup>26</sup> The experimental data give a less than linear dependence on  $N$  if no assumptions are made a priori. Bijsterbosch et al. measured the thickness and surface pressure of PS-PEO diblock copolymers at the air/water interface for various lengths of the PEO block.<sup>27</sup> The height of the PEO brush was found to scale as  $H \sim N^{0.8}$ .<sup>0.41</sup> Kent et al. used poly(dimethylsiloxane)-polystyrene (PDMS-PS) diblock copolymers with ethyl benzoate as the solvent. In this case the PS block is solvated and the PDMS block anchors the block copolymer to the interface.<sup>28-30</sup> They concluded that the thickness of the layer does not scale as  $H \sim N\sigma^{1/3}$ , but approximately as  $H \sim N^{0.86}\sigma^{0.22}$ .<sup>30</sup> In the same paper the behavior of the surface pressure of the PS brushes was investigated and compared with the predicted scaling law  $\pi \sim N\sigma^{5/3}$ . It was concluded that the scaling exponent of the surface pressure as a function of the density ranges from approximately 4.2 to 6.6, and increases slightly with  $N$ . In an elegant study Auroy et al. used NS to investigate PDMS end-grafted onto silica.<sup>31,32</sup> The brush height was observed to obey the scaling law. In this study, however, the grafting density could not be varied independently from the chain length.

Block copolymers adsorbing from a solvent onto a surface are commonly used to obtain densely grafted polymer layers. The grafting density depends on the length and characteristics of the adsorbing and nonadsorbing block, and on the solvent quality. A problem associated with adsorption from solution is that the polymeric surface density is not known during the experiment and has to be inferred from the experimental data. In the case of NR or NS this is done by fitting a model density profile to the reflectivity curve. This results in relatively high uncertainties in the surface density, especially at low coverage.<sup>33</sup> Such uncertainties can greatly influence the outcome of a power law fit, from which scaling exponents follow. Furthermore, it

is uncertain whether in practice the density of the adsorbed block copolymers is high enough to enter the brush regime. The relative coverage  $\sigma^*$ , defined as  $\sigma^* = \sigma 4\pi R_G^2$ , ranges in general from 2 to 10, where  $R_G$  is the three-dimensional radius of gyration. The onset of chain stretching occurs around  $\sigma^* \approx 2$ , and at low  $\sigma^*$  it is expected that the asymptotic brush regime is not reached. It is therefore our opinion that for nonadsorbing grafted polymers the scaling laws of the height and surface pressure as a function of the grafting density still await final experimental verification.

In the case of *attractive* surface-segment interactions the situation is even more complex. In this case a pancake structure is found at low grafting densities; the polymer optimizes its polymer-surface contacts by assuming a relatively flat conformation. With increasing grafting densities the chain is forced by steric interactions to protrude into the solution, and a brush is formed as the extent of displacement increases. Alexander investigated this "pancake-cigar" transition of grafted adsorbing chains using a simple scaling model. In this model the segment density profile of both states is taken to be a step function.<sup>5</sup> The model predicts the pancake-brush transition to be first-order, which is inferred from the observation that the chemical potential of the polymer chains is not a monotonically increasing function of the grafting density. A van der Waals loop for the chemical potential is found, corresponding with coexistence of two phases. The transition is reported to occur at a grafting density  $\sigma \approx R_G^{-2}$ .

A more refined scaling model, releasing the constraint of a uniform segment density, is used by Ligoure to analyze a similar system of grafted adsorbing polymers.<sup>34</sup> In this model the adsorbed polymer is represented as a distribution of loops, trains, and tails, and constitutes a so-called self-similar adsorbed layer (SSAL). A loop distribution is assumed beforehand, in which small loops and tails are neglected. The chemical potential is analyzed in a fashion similar to that in the paper of Alexander. It is concluded that the conformation transition from a SSAL to a quasi-brush with increasing grafting density is first-order under certain conditions. The density at which this transition is found is higher than the overlap density (i.e.,  $\sigma^* > 1$ ). The width of the phase coexistence regime is predicted to depend on the length of the chain and on the segmental adsorption energy. In a recent paper Aubouy et al. investigated a similar model, but they included the small loops and tails in the loop distribution. They concluded that the transition between the SSAL and a quasi-brush is continuous.<sup>35</sup> The polymer layer at relative densities exceeding unity consists of a SSAL close to the surface, and a polydisperse brush layer stretched outward from the surface. The grafting density at which the layer structure progressively changes is of the order of an adsorbed monolayer (i.e.,  $\sigma \sim (a^2 N)^{-1}$ , where  $a$  is the bond length). Several scaling relationships are given for quantities in this continuous transition, such as the chemical potential of the chain, the height of the layer, and the loop distribution as a function of the grafting density. Clearly, the mechanism of the pancake-brush transition varies with the assumptions made in the model. By postulating a functional form for the loop distribution Ligoure concludes that the brush is formed through gradual enlargement of the loops close to the surface (the proximal region). If no loop distribution is

assumed beforehand, the brush develops in the distal region by a gradual extension of the polymer tails and, simultaneously, a gradual diminishment of the SSAL.

Experimentally, a first-order adsorption–desorption transition of a polymeric system at a surface was reported for the adsorption of PEO triblock copolymers with a hydrophobic center block on PS spheres.<sup>36</sup> The transition was characterized by a plateau in the measured hydrodynamic radius of the coated spheres. A more exact manner to determine the nature of the adsorption–desorption transition of either grafted chains or chains with strongly adsorbing end groups is a measurement of the surface pressure as the grafting density is increased. A plateau of constant surface pressure indicates the coexistence of two polymeric phases, the ratio of which depends on the grafting density, and thus a first-order transition. This is comparable to the constant surface pressure of a surfactant monolayer during the (first-order) liquid-expanded–liquid-condensed phase transition. Such a possible transition can be investigated experimentally by compressing block copolymers adsorbed at an air/solvent interface in a Langmuir trough. The surface pressure resulting from both the solvated and nonsolvated blocks is measured as a function of the continuously changing grafting density. Bijsterbosch et al. investigated with this technique the properties of diblock PS–PEO at the air/water interface.<sup>27</sup> The short PS blocks act as inert anchors and do not contribute to the surface pressure. The long PEO chains are water-soluble but also adsorb at the air/water interface.<sup>37</sup> A grafting density regime is reported in which the surface pressure of the polymer layer increases slowly. The observed density at which this semiplateau is found corresponds roughly to that of an adsorbed polymeric monolayer. This semiplateau is attributed to the gradual desorption of the PEO chains from the air/water interface. No coexistence regime is reported, nor any other feature characteristic of a first-order phase transition.

In this paper we examine the properties of grafted polymers with and without surface affinity in a good solvent with a numerical SCF model. In this model all possible polymer conformations are taken into account. This approach differs from a scaling or analytical SCF model, in which solely the most probable conformations are considered. The results of the surface pressure measurements of the PS–PEO system by Bijsterbosch et al.<sup>27</sup> are used to verify the validity of the numerical results. We will concentrate on the transformation of the layer from an adsorbed to a partially desorbed structure when the grafting density is increased. As phase transitions are characterized by the behavior of thermodynamic quantities such as the chemical potential and its derivatives, special attention is given to these quantities. Such an approach yields information on the mechanism of adsorption–desorption and the classification of this transition. A comparison is made with the mean-field theory of phase transitions, especially with scaling relationships for thermodynamic parameters near a critical point. Taking the adsorption of the PEO chains to the interface into account, we also reexamine the experimental results of Bijsterbosch et al. The scaling behavior of the surface pressure and height of a brush as a function of the grafting density is investigated.

The outline of the remainder of this paper is as follows. In section 2 a brief description is given of the

applied SCF model. In section 3 the numerical results for the surface pressure of grafted polymers with and without surface affinity are presented, and these results are compared with the experimental data of Bijsterbosch et al. The power law dependencies of both the numerical and experimental results are examined. In section 4 the pancake–brush transition of grafted adsorbing polymers is investigated in detail. In particular, the behavior of the chemical potential of the grafted chains in the proximity of the adsorption–desorption transition is considered as a function of the segment–surface interactions and the chain length. In section 5 we summarize our results and conclusions.

## 2. Self-Consistent Field Model

The properties of neutral, linear polymers end-grafted on a surface are investigated using the numerical SCF model of Scheutjens and Fleer.<sup>38,39</sup> The equilibrium distribution of the polymers is calculated taking all possible conformations into account, weighted by the Boltzmann probability factors. A short review of the underlying principles is given; a more extensive treatment can be found in the literature.<sup>7</sup>

A cubic lattice is considered, consisting of  $M$  layers, numbered  $z = 1, 2, \dots, M$ , where  $z$  is the distance to the surface measured in units of the thickness of a lattice layer,  $a$ . Each lattice layer consists of  $L$  sites of volume  $a^3$ , and each site is occupied by either a polymer segment or a solvent entity. The system is incompressible, which implies that the sum of the densities of all segment types is unity in each layer. As we consider grafted chains immersed in a pure solvent, the solvent density in the bulk is unity. We stress that the polymer chains therefore do not have a chemical potential defined by a bulk concentration. The polymer chains are  $N$  segments long and are end-grafted with a grafting density  $\sigma = n_p/L$ , where  $n_p$  is the total number of grafted chains. End-grafted in this case simply defines the probability of the first segment to reside in the first layer to be unity. In the mean-field approximation the segment density in each layer is considered to be laterally uniform, and the dimensionless polymer segment density  $\rho(z)$  is solely a function of the distance to the surface. This also entails the grafted chains to retain translational entropy along the grafting surface. Flory–Huggins parameters  $\chi_{ij}$  account for nearest-neighbor interactions between segments  $i$  and  $j$ . The potential energy, in units of  $kT$ , of a solvent entity is given as

$$u_0(z) = -\ln(1 - \rho(z)) \quad (1)$$

whereas that of a polymer segment is

$$u'(z) = -\ln(1 - \rho(z)) - 2\chi\langle\rho(z)\rangle + \delta(z,1)(\chi_{\text{sur}} - \lambda_1\chi) \quad (2)$$

The angular brackets  $\langle\rho(z)\rangle$  denote the weighted average of nearest-neighbor contacts in the layers  $z-1$ ,  $z$ , and  $z+1$ :  $\langle\rho(z)\rangle = \lambda_1\rho(z-1) + \lambda_0\rho(z) + \lambda_1\rho(z+1)$ . For a cubic lattice,  $\lambda_0$  and  $\lambda_1$  equal  $4/6$  and  $1/6$ , respectively. The  $\chi$  parameter accounts for the polymer–solvent interactions,  $\chi_{\text{sur}}$  for those of the polymer with the surface. In the definition of  $\chi_{\text{sur}}$  it is taken into account that the number of contacts between the surface and the polymer segment is a factor  $\lambda_1$  smaller than the number of contacts between the polymer segment and the solvent. Thus, the definition of  $\chi_{\text{sur}}$  is similar to that of Silber-



berg, besides a difference in sign.<sup>40</sup> The  $\chi$  for solvent-surface interactions is set equal to zero. The logarithmic term in eqs 1 and 2 is the mixing entropy of the solvent; the conformational entropy of the polymer chain is taken into account in the following chain statistics.

The conformations of the polymer chains in the local field are expressed in terms of a two-point correlation function  $G(z,z';s)$ , which is the joint probability of a chain of  $s$  steps having segment  $s' = 1$  in layer  $z$  and segment  $s' = s$  in layer  $z'$ , taking all possible configurations into account. To this end the segment weighting factor is defined as the Boltzmann distribution of a single detached segment in layer  $z$ :

$$G(z) = \exp(-u'(z)) \quad (3)$$

Because of the connectivity of the chain segments, the distribution of a segment depends on that of its neighbors; in the case of a segment  $s$  located in layer  $z$ , segment  $s - 1$  must be located in the layers  $z - 1$ ,  $z$ , or  $z + 1$ . This results in a recurrence relationship in which  $G(z,z';s)$  is expressed in terms of a chain which is one segment shorter in length:

$$G(z,z';s) = \langle G(z,z';s-1) \rangle G(z') \quad (4)$$

where  $\langle G(z,z';s-1) \rangle$  denotes a weighted average as defined above. In the case of grafted chains the grafting gives a restriction for the first segment in the form of a Dirac function. The probability of segment  $s$  residing in layer  $z'$  is furthermore recognized as the joint probability of the end segment of a chain of length  $s$  and that of a chain of length  $(N - s + 1)$  residing in layer  $z'$ , corrected for a double counting of  $G(z')$ . In the case of grafted chains the grafting restriction applies for one of the chain parts. The density of segment  $s$  of a chain of length  $N$  in layer  $z'$  is therefore

$$\rho(z',s) = C \frac{G(1,z';s) \sum_z G(z',z,N-s+1)}{G(z')} \quad (5)$$

The normalization constant  $C$  is found using the fact that the grafting density is fixed. The density of each segment summed over all layers must equal the grafting density and thus

$$C = \frac{\sigma}{\sum_z G(1,z,N)} \quad (6)$$

The total polymer density in layer  $z$ , for a given segment potential field  $u'(z)$ , is given by summation of  $\rho(z,s)$  over all chain segments,  $s = 1 \dots N$ . The resulting density must be consistent with the potential fields expressed by eqs 1 and 2 for all  $z$ . The solution is generated by numerical iteration.

Besides structural properties of the grafted polymers, we are interested in the thermodynamic properties of the system. To examine the behavior of the surface pressure of the grafted polymers as a function of the grafting density, it is necessary to determine the excess free energy of the layer. This quantity, denoted by  $\Delta$ , consists of two terms; an entropic contribution which takes all polymer configurations with the corresponding probabilities into account, and an enthalpic contribution which is a function of the densities in combination with

the  $\chi$ -parameters. In general,  $\Delta$  is given as (per unit area, in units kT)<sup>41</sup>

$$\Delta = G - \sum_b n_b \mu_b = \sigma \ln \left\{ \frac{\sigma N}{\sum_z G(1,z,N)} \right\} - \sum_{z,i} \rho_i(z) u_i(z) + \frac{1}{2} \sum_{z,i,j} \rho_i(z) \chi_{ij} \langle \rho_j(z) \rangle \quad (7)$$

where  $G$  is the total Gibbs free energy of the system and  $\sum_b$  denotes the sum over all components that are exchanged with the bulk. In the case of a grafted polymer in a pure solvent this reduces to

$$\Delta = \sigma \ln \left\{ \frac{\sigma N}{\sum_z G(1,z,N)} \right\} + \sum_z \ln(1 - \rho(z)) + \sum_z (\chi \rho(z) \langle \rho(z) \rangle - \frac{1}{2} \chi \lambda_1 \rho(z) \delta(z,1)) \quad (8)$$

In the derivation of this equation, we make use of the fact that the term  $\sum_z \frac{1}{2} \chi (\rho(z) - \langle \rho(z) \rangle) = \frac{1}{2} \chi \lambda_1 \rho(z) \delta(z,1)$ , as the sum is taken over the total grafted layer. It is evident that, if all  $\chi$ -parameters are set to zero, eq 8 reduces to a similar expression derived by Martin and Wang.<sup>10</sup>

$$\Delta = \sigma \ln \left\{ \frac{\sigma N}{\sum_z G(1,z,N)} \right\} - \sum_z u_0(z) \quad (9)$$

Both the chemical potential of the grafted chains and the surface pressure of the system contribute to  $\Delta$ . The surface pressure is defined as (kT per unit area)

$$\pi \equiv \left( \frac{\partial G}{\partial A} \right)_{T,N_p,N_s} \quad (10)$$

where  $G$  is the total free energy and  $A$  is the total area. In a lattice model the grafting density is varied whereas the total volume and area are constant. The total free energy is replaced by the excess free energy, as the bulk contribution of the pure solvent is zero. The excess free energy consists of a contribution of the chemical potential of the grafted chains, and a contribution of the surface pressure due to the grafted chains. The first term is equal to  $\sigma(\partial\Delta/\partial\sigma)$ . The surface pressure of grafted chains in a pure solvent in the lattice model is therefore

$$\pi = \sigma \left( \frac{\partial \Delta}{\partial \sigma} \right)_{T,A,\mu_s} - \Delta \quad (11)$$

Carignano and Szleifer reported an analytic expression for  $\pi$  using a similar SCF model.<sup>8</sup> According to these authors the surface pressure can be explicitly calculated from the segment density profiles and the interaction parameters for a given grafting density  $\sigma$ . We believe their method to be incorrect, as explained in the Appendix. It is therefore necessary to obtain the derivative of the excess free energy with respect to the grafting density by numerical central differentiation, as was

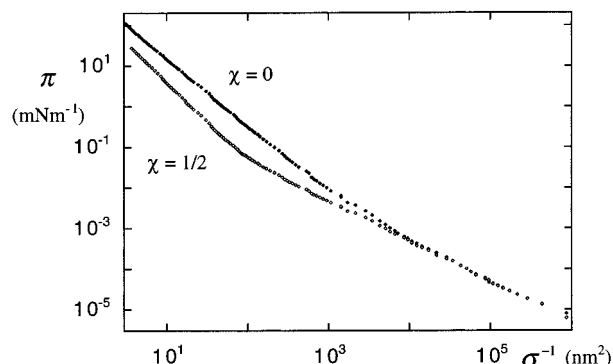


**Figure 1.** Lateral pressure  $\pi$  in the SCF model of grafted nonadsorbing polymers as a function of the area per chain in  $\text{nm}^2$ ,  $\sigma^{-1}$ , on a double-logarithmic scale. Two solvent conditions are shown:  $\chi = 0$  (good solvent) and  $\chi = 1/2$  ( $\Theta$  solvent). The scaling exponents at high densities are  $5/3$  and 2, respectively. Chain length  $N = 700$ , lattice cell length  $a = 0.35$  nm.

done previously by Martin and Wang.<sup>10</sup> In the following section we return to this point.

### 3. Grafted Adsorbing Polymers

In this section the SCF results for the surface pressure of grafted chains are presented and compared with experimental results. In Figure 1 the surface pressure isotherm of nonadsorbing grafted chains containing 700 segments for a good and  $\Theta$  solvent is presented in a double-logarithmic plot. The length of a lattice cell,  $a$ , is set 0.35 nm. This is equal to the PEO segmental length which facilitates comparison with experimental data.<sup>42</sup> The  $\chi_{\text{sur}}$  is set zero for both solvent qualities. At low densities the surface pressure scales linearly with the grafting density and is independent of the solvent quality. This is the expected ideal gas behavior for noninteracting coils. Carignano and Szleifer found a quadratic dependence of the surface pressure on the grafting density at very low densities. This is physically unrealistic and must be attributed to their incorrect expression for the surface pressure.<sup>8</sup>

For a good solvent ( $\chi = 0$ ) the power law exponent at high densities is  $5/3$ , as predicted by the analytical SCF model.<sup>6,19,43</sup> The crossover between the mushroom and the brush regime is found at relatively low densities, corresponding approximately to  $\sigma^* = 1$  (the equivalent area per chain is about  $1000 \text{ nm}^2$ ). As the solvent quality decreases, the crossover between the coil and brush regime is found at higher densities, and the power law exponent at high densities increases. This is in accordance with the fact that as the solvent quality decreases, the polymers are less stretched in the solvent and higher order virial interactions between segments become increasingly important. In a  $\Theta$  solvent ( $\chi = 0.5$ ) the linear scaling of the surface pressure is found up to relatively high grafting densities. At high densities the power law exponent equals 2. This is the expected exponent in the case that the brush properties are predominantly determined by third-order virial interactions, as is predicted by analytical SCF models.

The surface pressure isotherms of grafted adsorbing polymers are given for several chain lengths in Figure 2. The polymers have an attractive adsorption energy of 1 kT per segment,  $T = 298$  K,  $a$  is again 0.35 nm, and  $\chi$  is set to zero. This represents a grafted polymeric system in a good solvent with an appreciable surface affinity. SCF density distributions of grafted adsorbing polymers by Bijsterbosch et al. presented the following

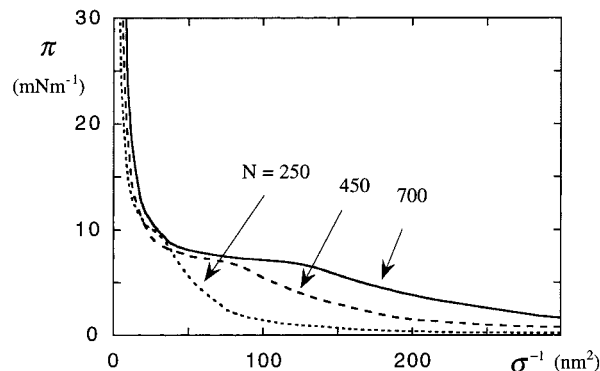


**Figure 2.** SCF surface pressure isotherms of grafted adsorbing chains as a function of the area per chain in  $\text{nm}^2$ ,  $\sigma^{-1}$ , on a linear scale. Chain lengths are  $N = 250$ , 450, and 700,  $a = 0.35$  nm,  $\chi = 0$ , and  $\chi_{\text{sur}} = -1$ .

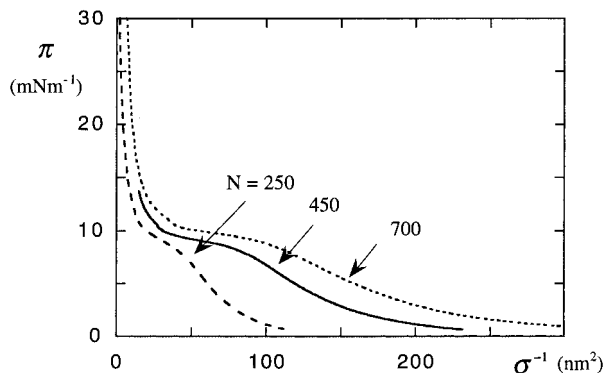


**Figure 3.** Experimental surface pressure as a function of the area per chain in  $\text{nm}^2$ ,  $\sigma^{-1}$ , for PS-PEO block copolymers at the air/water interface. PEO lengths are 250, 450, and 700. The data are taken from ref 27.

picture.<sup>27</sup> At low densities the polymers have a pancake conformation due to attractive interactions with the surface; nearly all segments are close to the surface. At a sufficiently high grafting density the monolayer at the surface is filled, and excess segments are forced into the solvent by steric interactions. The grafting density at which this transition takes place is approximately  $\sigma \sim (Na^2)^{-1}$ . At higher densities an increasing fraction of segments is in the solvent phase and gradually a brush is formed. We note that in the brush regime the segment density in the monolayer at the surface remains close to unity. The density distributions correlate with the numerical surface pressure isotherms. At low grafting densities the surface pressure increases strongly, because of the filling of the monolayer next to the surface. When  $\sigma \sim (Na^2)^{-1}$ , a semiplateau is found during the pancake-brush transition in which the surface pressure increases gradually but continuously with an increasing grafting density. At high grafting densities the surface pressure increases strongly as a result of interacting brushes. The adsorption-desorption transition is continuous in our numerical calculations. This is also evident from the fact that the chemical potential of the polymers is a monotonically increasing function of the grafting density (not shown).

In Figure 3 experimental isotherms of PS-PEO block copolymers at the air-water interface, measured by Bijsterbosch et al., are presented.<sup>27</sup> The block copolymers consist of short PS blocks which act as inert anchors, and PEO tails of lengths identical to those used in Figure 2. The polymers are deposited on the air/water interface from a volatile apolar solvent. The surface

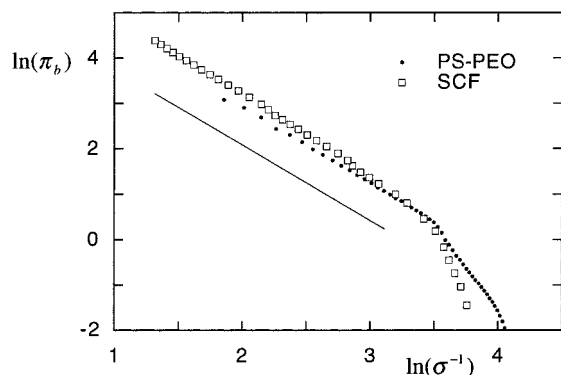


**Figure 4.** Lateral pressure of the brush,  $\pi_b = \pi - \pi_{\text{pla}}$ , as a function of the area per chain in  $\text{nm}^2$ ,  $\sigma^{-1}$ , on a double-logarithmic scale. Both SCF and experimental results are shown for  $N = 700$ . A line corresponding with a scaling exponent  $5/3$  is drawn as illustration. The PEO value for  $\pi_{\text{pla}}$  is  $9.8 \text{ mN m}^{-1}$ ; that for the SCF data is  $8.2 \text{ mN m}^{-1}$ .

pressure of the block copolymers is measured continuously at room temperature as the layer is compressed in a Langmuir trough. The  $\Theta$  temperatures of PEO in water are reported as  $\Theta_- = -12^\circ \text{C}$  (UCST) and  $\Theta_+ = 96^\circ \text{C}$  (LCST), indicating that water at room temperature is a good solvent.<sup>44</sup> The adsorption energy per PEO segment is deduced from the value of  $\pi$  in the adsorption-desorption plateau ( $9.6\text{--}9.8 \text{ mN m}^{-1}$ ). This is the sum of the effective adsorption energy per segment ( $\pm 0.4 \text{ kT}$ ) and the critical adsorption energy per segment ( $0.2 \text{ kT}$ ). As the air/water interface is not perfectly sharp, an additional entropic contribution must be taken into account. The effective adsorption energy is therefore somewhat more than  $0.6 \text{ kT}$  per segment.

A comparison of Figures 2 and 3 shows that the SCF model is in semiquantitative agreement with the experimental data, particularly at high densities. The shape of the numerical isotherm, especially the adsorption-desorption plateau occurring at a surface pressure of approximately  $8 \text{ mN m}^{-1}$  in Figure 2, corresponds well with that of the experimental isotherm. Both the numerical and the experimental isotherms show a continuous increase in  $\pi$  with a decreasing area per molecule (i.e., increasing  $\sigma$ ). This indicates that the continuous adsorption-desorption transition is modeled in a correct manner. A slightly smaller value for  $a$  could be used to match the experimental and numerical isotherms more accurately. The value for the PEO segment length as reported in the literature nevertheless gives a very satisfying agreement. At low densities the behavior is qualitatively correct but the quantitative agreement is less satisfactory. This is characteristic in general for mean-field models, which cannot cope with lateral inhomogeneities such as pancakes.

At grafting densities above the adsorption-desorption transition density the surface pressure is considered to consist of two contributions: a constant pressure  $\pi_{\text{pla}}$  resulting from a monolayer of adsorbed segments of constant density and an increasing surface pressure  $\pi_b$  due to the formation of a brush. The plateau value  $\pi_{\text{pla}}$  corresponds to the saturated pressure of the adsorbed homopolymer. Experimentally, the saturated surface pressure of a PEO solution is reported to be equal to  $9.8 \text{ mN m}^{-1}$ , indicating that the additional surface pressure upon compression is indeed due to brush formation.<sup>37</sup> For the numerical SCF isotherm the value of the semiplateau is estimated to be  $8.2 \text{ mN m}^{-1}$ . In Figure 4 the surface pressure of the brush,  $\pi_b = \pi -$

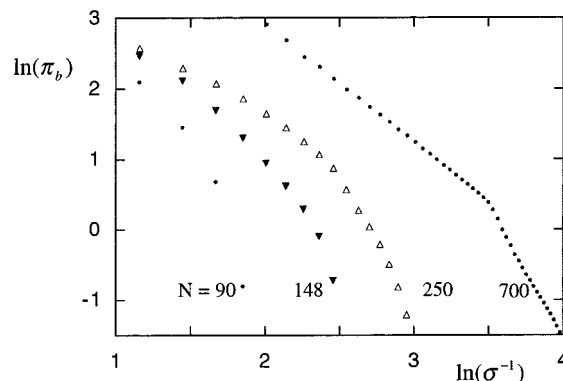


**Figure 5.** Lateral pressure of the PEO brush in a fashion similar to Figure 4 for various PEO chain lengths. Chain lengths shown are  $N = 90, 148, 250$ , and  $700$ . The value of  $\pi_{\text{pla}}$  is the same as that in Figure 4.

$\pi_{\text{pla}}$ , is plotted double logarithmically against the area per chain for  $N = 700$ , both for the experimental and for the SCF data. A line corresponding to a power law exponent of  $5/3$  is drawn for comparison. The exponent found at high densities equals approximately the value predicted by scaling relationships of SCF models. The exact exponent depends slightly on the choice of the plateau value;  $\pi_{\text{pla}}$  taken to be  $9.6 \text{ mN m}^{-1}$  gives  $1.58$  as an exponent,  $9.8$  gives  $1.67$ , and subtracting  $10 \text{ mN m}^{-1}$  results in  $1.78$ . Nevertheless, the experimentally measured surface pressure of the PEO brush at high densities corresponds with the scaling predictions for SCF models and can be reproduced successfully with the numerical SCF theory.

We note that the surface pressure  $\pi_b$  of the PEO brush increases very fast in the double-logarithmic plot at low densities (see Figure 4). This is an artifact resulting from the necessary subtraction of  $\pi_{\text{pla}}$ . At total surface pressures slightly larger than  $\pi_{\text{pla}}$  the value of  $\pi_b$  is close to zero. A small increase in  $\pi_b$  results in a large increase in a double-logarithmic plot. Physically, this merely signifies that the grafting density, with respect to the transition density, is not high enough for a brush to be formed.

It is of interest to examine whether this scaling behavior is reproduced by all PEO chain lengths. In Figure 5 the surface pressure for chain lengths  $90, 148, 250$ , and  $700$  is plotted in a fashion similar to that in Figure 4. It is found that a regime with a constant power law exponent, as observed both experimentally and numerically for  $N = 700$ , is not present in the experimental isotherms of short PEO chains. A regime with a constant exponent is found for PEO chains of  $450$  segments, if the plateau value is taken to be slightly lower,  $\pi_{\text{pla}} = 9.2 \text{ mN m}^{-1}$  (not shown). This observation agrees with the experimental finding that in this molecular-weight regime the saturated surface pressure of a PEO homopolymer increases with increasing molecular weight.<sup>37</sup> The extent of the regime of constant exponent for  $N = 450$  is less than that of  $N = 700$ . These results show that scaling relationships should be verified experimentally with sufficiently long chains. In light of this, it is questionable whether MC and MD simulations are suitable to examine polymer properties in the brush regime.<sup>11,12</sup> The chain length used in these studies is often not more than  $50$  segments which leads to higher power law exponents with narrow regimes of constant scaling. We conclude that scaling relationships for the asymptotic brush regime, based on the assump-



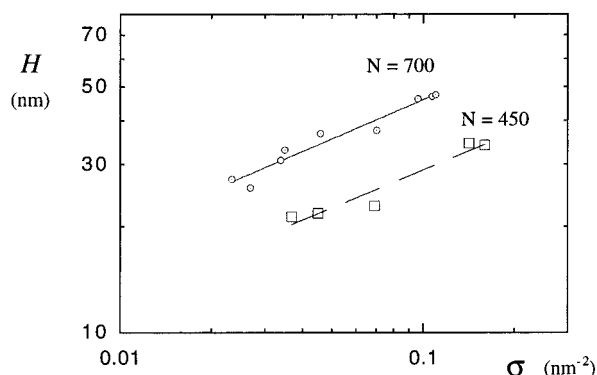


**Figure 6.** Height of the PEO brushes (in nm) for  $N = 450$  and  $700$  as a function of the number of chains per unit area,  $\sigma$  ( $\text{nm}^{-2}$ ), on a double-logarithmic scale. The corresponding scaling exponents are  $0.35$  and  $0.33$ , respectively.

tion that either second or third virial interactions dominate the properties of the brush, should be tested numerically and experimentally for sufficiently long chains.

With the above results in mind, we reexamine the experimental NR data for the thickness of the PS-PEO brushes. Bijsterbosch et al. combined the results for the thickness of the polymer layer at high densities in one plot, regardless of the chain length.<sup>27</sup> The fitted power law for  $H/N$  versus  $\sigma$  yielded the exponent  $0.41$ , somewhat higher than the predicted  $1/3$ . The analysis of the surface pressure isotherms, however, demonstrates that only long chains are expected to be truly in the asymptotic brush regime. In Figure 6 the measured thickness for PEO chains of  $450$  and  $700$  segments is plotted double logarithmically as a function of the number of chains per unit area. Fitting these results to a power law yields an exponent of  $0.33$  for  $N = 700$  and  $0.35$  for  $N = 450$ . Again, the analytical SCF model correctly predicts the experimental behavior of the polymer brush, provided long chains at high grafting densities are used.

The question arises why the results of our SCF model and the experimental PS-PEO system are in good agreement with analytical SCF models, whereas in the literature it is reported that such agreement does not exist.<sup>22,28-30</sup> It is evident that the grafting density and surface affinity of the grafted chains must be dealt with in a proper manner to investigate power law dependencies of the surface pressure and brush height. As the subtraction of the saturated surface pressure of PEO demonstrates, it is necessary to know the adsorption behavior of the anchored block and the contribution of the anchoring block to interpret the total surface pressure. We remark that the small polystyrene blocks used by Bijsterbosch et al. are known not to wet the surface; their contribution to the surface pressure has been checked and is zero at the measured surface densities. The measured surface pressure can therefore be completely ascribed to the PEO chain, and at high densities safely separated into a contribution due to adsorption and a contribution due to solvation. In the case of block copolymers with anchoring blocks that wet the surface or large compared to the bouy block, the interaction between the anchoring block, solvent interface, and solvated block is not known. The assumption is usually made that such activity is negligible. The surface pressure of the brush however is the difference between total surface pressure and the surface contributions of

the anchoring block and the anchored block combined. It is thus clear that the scaling of the surface pressure of a brush cannot be examined in a reasonable manner without correcting for adsorption effects.

Another problem is the determination of the amount of polymer on the surface. Bijsterbosch et al. deposited the PS-PEO block copolymer on the air/water interface using chloroform as a solute. Both chloroform and PS are highly hydrophobic and when deposited from the air do not mix with water. The deposited amount is therefore known within a reasonable accuracy. In contrast, Kent et al. used either a polymer solute of higher density than the organic bulk phase or dry block copolymer.<sup>28-30</sup> Because of loss of the polymer during deposition, the polymeric density is not known during the experiment and is determined via integration of the neutron reflectivity curves. This is less accurate, in particular at low polymeric densities.<sup>33</sup> Such inaccuracy is particularly important when the surface pressure or layer thickness is measured as a function of the grafting density and fitted to a power law. Verification of the scaling law between the layer height and grafting density is thus difficult, when both parameters are determined by NR and are consequently sensitive to experimental uncertainties.

In a recent paper Richards et al. investigate the poly-(dimethylacrylate)-poly(ethylene oxide) (PDMA-PEO) block copolymer at the air/water interface with NR.<sup>33</sup> At the examined densities the PEO was found to have a rather flat structure which extended only slightly into the water phase. No agreement between the reflection spectrum and parabolic density profiles was obtained. Richards et al. concluded that the brush structure, as reported by Bijsterbosch et al., is erroneous. According to the authors the PEO layers collapse before the brush regime is obtained. At the densities examined ( $1.2 \text{ mg/m}^2$ ) the measured surface pressure of the PDMA-PEO layer is of the order  $5 \text{ mN m}^{-1}$ . In the PDMA-PEO isotherm this density is halfway in the adsorption-desorption plateau. The structure thus corresponds nicely to the partly desorbed pancake conformation in our analysis. Parabolic density profiles are evidently not expected at such grafting densities. However, the highest density used for the PS-PEO of length  $N = 700$  is  $6 \text{ mg/m}^2$  at a surface pressure of the order  $25 \text{ mN m}^{-1}$ , which is well beyond the adsorption-desorption plateau and in the brush regime.

We believe, therefore, that detailed knowledge of the adsorption properties of the block copolymers is essential for the correct interpretation of experimental results. Surface pressure isotherms in combination with the SCF model can be analyzed for identification of the polymer conformation at a given grafting density. Such identification is necessary for the interpretation of NR results. Moreover, the power law of the surface pressure in the brush regime as predicted by analytical SCF models is only found if three conditions are met: (i) The grafting density  $\sigma$  has to be known exactly because of the strong dependence of  $\pi$  on  $\sigma$ ; (ii) all contributions due to surface affinity of both the solvated and nonsolvated block have to be known and subtracted from the total surface pressure, as these do not contribute to the surface pressure of the solvated brush; (iii) long chains at high densities are necessary to obtain the power law corresponding to the asymptotic brush regime. Especially this last condition is very important: if it is not

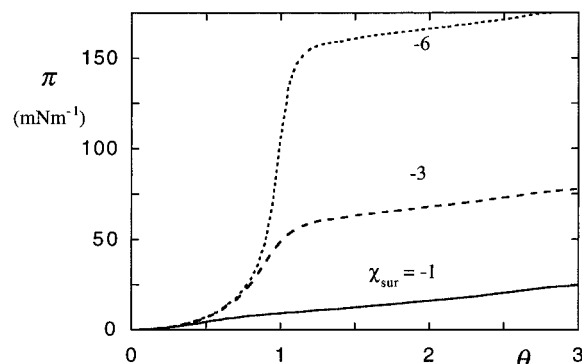


**Figure 7.** SCF surface pressure isotherms of grafted adsorbing polymers as a function of the total polymer density  $\theta$  for  $N = 50$ . The segmental adsorption energies used are  $\chi_{\text{sur}} = -1, -3$ , and  $-6$ .

satisfied, a regime with a constant scaling exponent cannot be expected to be found.

#### 4. Pancake–Brush Transition

In the previous section it was shown that the numerical SCF model correctly models the adsorption–desorption mechanism of the PS–PEO block copolymers, the so-called pancake–brush transition. In this section we consider the adsorption–desorption transition of grafted polymers for varying adsorption energies and chain lengths in a good solvent; unless specified otherwise the  $\chi$  is set zero (an athermal solvent). The transition is expected to become increasingly abrupt as the interaction between the segments and the surface becomes more attractive. Also, with increasing adsorption energies the total polymer density at which the transition takes place is expected to progressively mirror an adsorbed monolayer of unity density. It is especially interesting to investigate whether the transition becomes first-order in certain regimes or whether it remains continuous throughout.

The behavior of the surface pressure for various adsorption energies is plotted in Figure 7 for a constant chain length ( $N = 50$ ). On the x-axis the total polymer density  $\theta$  is plotted. The adsorption energies used are  $-1, -3$ , and  $-6$  kT per segment. For high adsorption energies, the surface pressure of the adsorbed grafted chains changes abruptly around the transition density ( $\theta \approx 1$ ). Below this density the surface pressure has a low value corresponding to that of a partially filled monolayer; above it one finds a semiplateau value corresponding to a monolayer of constant density and partially desorbed chains. The height of the plateau evidently depends on the adsorption energy. With increasing grafting densities (not shown in Figure 7) the surface pressure of the brush develops, and eventually the isotherms for different adsorption energies merge, as the pressure of the brush dominates the constant contribution of the monolayer.

A suitable quantity for examining the behavior of the system during this transition is the chemical potential of the grafted chains. As mentioned in section 2, the chemical potential of the grafted chains is not defined by a bulk concentration. It can be determined from the change in excess free energy with changing grafting density. Therefore  $\mu$  is a thermodynamic function of an independent field,  $\sigma$ . In Figure 8 the segmental chemical potential  $\mu/N$  is plotted against the total polymer density

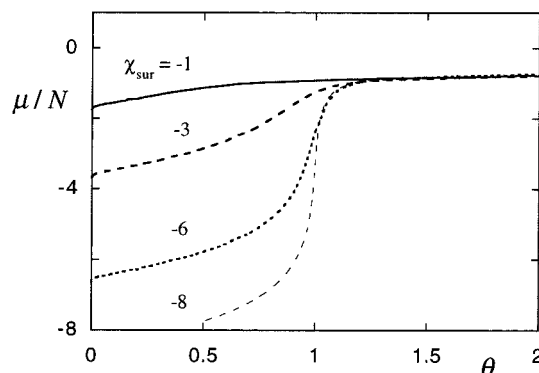


**Figure 8.** The chemical potential per segment of grafted adsorbing polymers as a function of the total polymer density for various adsorption energies.  $N = 50$  and  $\chi_{\text{sur}} = -1, -3, -6$ , and  $-8$ .

$\theta$  for  $N = 50$  and various adsorption energies. Below the transition density ( $\theta \approx 1$ ) the chemical potential is a function of the adsorption energy as the newly introduced polymer can adsorb at the surface. Above the transition density it is independent of the adsorption energy; the filled monolayer gives a constant contribution to the free energy and the chemical potential in this regime depends only on the chain length and the solvent conditions. The abruptness of the transition is illustrated by the behavior of the chemical potential around  $\theta = 1$  at a high adsorption energy. The transition remains continuous, however, as demonstrated by the continuous increase in the chemical potential with an increasing grafting density.

The behavior of the chemical potential of the grafted chains suggests that for densities greater than unity the evolution of the polymer configuration is independent of the adsorption energy. For a density as low as  $\theta \sim 1.2$  the chemical potential is virtually equal for all adsorption energies. As the chemical potential is defined as the change in excess free energy with increasing grafting density, the adsorbed monolayer gives a constant contribution to the excess free energy, and the chemical potential is determined by the increasing polymeric density in the solvent phase. This indicates that the grafted polymer layer consists of a collapsed monolayer of constant density at the surface and a number of tails sticking out into the solvent phase. Moreover, the entropic contribution of the desorbed polymer is independent of the adsorption energy (the enthalpic part of the excess free energy is zero as  $\chi$  is set to zero). This agrees with the picture of the brush formation being initiated in the distal part of the polymer layer (i.e., by the tails). This mechanism also excludes a significant role for loops in the proximal part of the adsorbed layer, as a dependence of the loop distribution on the adsorption energy would translate itself in a similar dependence of the chemical potential.

Aubouy et al. carefully investigated the regime above the overlap density (i.e.,  $\theta \geq 1$ ).<sup>35</sup> In this model the adsorption of grafted chains is represented as a distribution of loops and tails, and the excess free energy is evaluated with scaling arguments. In the case that the monomer density at the surface is of order unity it is concluded that the polymer layer close to the surface is similar to that of a purely adsorbed layer, whereas in the distal region it resembles a polydisperse brush. They further derive that the chemical potential in this regime scales as  $\mu \sim \sigma^{5/6}$ . Such a power law is not found in our



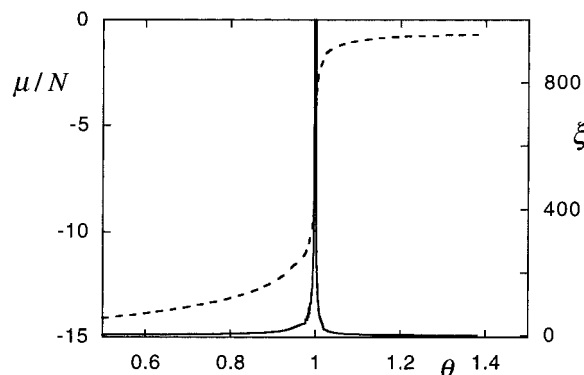


**Figure 9.** Behavior of the chemical potential per segment of the grafted adsorbing chains and its derivative with respect to the density for a high adsorption energy.  $N = 50$  and  $\chi_{\text{sur}} = -14.5$ .

SCF results. In other respects the physical picture of the scaling approach and the SCF analysis are in good agreement. We believe that the model of Aubouy et al. correctly predicts a continuous transition with an increasing density. The emphasis on the gradual disappearance of the loop distribution is, however, not observed by our SCF model.

It is instructive to classify the class of the pancake-brush phase transition, and to relate it to other phase transitions in well-studied systems. For this purpose the chemical potential is recognized as a suitable order parameter, and the grafting density as an external field parameter. Every thermodynamic parameter that is zero in a disordered phase (nonadsorbed conformation) and nonzero in an ordered (adsorbed conformation) phase can be denoted an order parameter. In an Ising model the analogous quantities are the magnetization and the external magnetic field. As  $\chi_{\text{sur}}$  is a temperature-dependent parameter, and the transition becomes sharper with increasing adsorption energies, the analogy with the reciprocal temperature in an Ising model is reasonable. We are interested in whether the pancake-brush transition remains continuous under all circumstances in a good solvent. In other words, is the system always found above the critical temperature, or can a set of variables (chain length, adsorption energy) be found for which the change in chemical potential is discontinuous? The latter behavior is characteristic for a first-order transition, for instance, the nonzero magnetization of a ferromagnet in a zero field below the critical temperature.

In Figure 9 the chemical potential per segment and its derivative with respect to the density,  $N^{-1}(\partial\mu/\partial\theta)$ , are plotted around the critical polymer density. The length of the chain is 50 segments; the adsorption energy  $\chi_{\text{sur}} = -14.5$ . The chemical potential remains a continuous increasing function of the grafting density; its derivative with respect to the polymeric density at  $\theta = 1$  is close to divergence. This derivative is interpreted as a segmental conformational susceptibility and is denoted by  $\xi$ . This quantity is a measure for the overall change in polymer structure with varying density. It is evident that the near-divergence of  $\xi$  denotes a strong change in conformation around  $\theta = 1$ . The curve of the chemical potential is similar to that of the magnetization  $M$  of a ferromagnet as a function of the external field  $H$  at a temperature slightly above the critical temperature. In this case the magnetization changes strongly with small changes in  $H$  around  $H =$

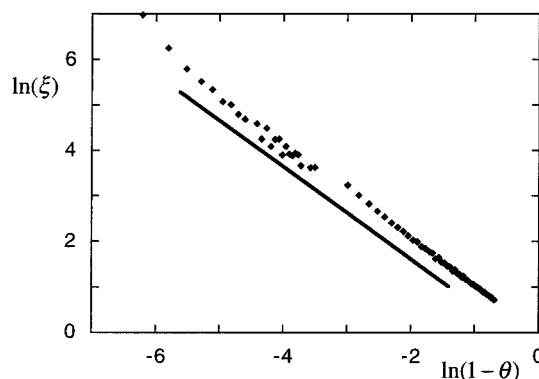


**Figure 10.** Scaling behavior of the segmental conformational susceptibility,  $\xi$ , as a function of the reduced density  $1 - \theta$  in the proximity of the critical density  $\theta = 1$ . A line corresponding to the scaling exponent  $-1$  is drawn as illustration.  $N = 50$  and  $\chi_{\text{sur}} = -14.5$ .

0. Consequently, the curve of  $\xi$  is similar to the so-called  $\lambda$ -curve of the susceptibility of a ferromagnet,  $\chi \equiv (\partial M / \partial H)_T$ , at a temperature close to the critical temperature. Such behavior is a fingerprint of a continuous transition approaching the critical point.<sup>45,46</sup>

The theory of phase transitions and the renormalization theory of critical phenomena describe the behavior of thermodynamic quantities in the vicinity of a critical point. The majority of the derived relationships accounts for the behavior of such quantities at the critical point; an exception is the derivative of the order parameter with respect to an external field parameter at constant temperature close to the critical temperature, for example the magnetic susceptibility or in our case  $\xi$ . In a magnetic system the magnetic susceptibility changes strongly around zero external field; in the pancake-brush transition  $\xi$  changes strongly around  $\theta = 1$ . According to renormalization theory the scaling exponent of these quantities as a function of the external field parameter for small values of the external field equals  $-1$  in a mean-field model, both above and below the critical temperature.<sup>46</sup> In Figure 10  $\xi$  is shown for  $\chi_{\text{sur}} = -14.5$  and  $N = 50$  in a double-logarithmic plot as a function of the reduced density  $(1 - \theta)$ . A line with an exponent  $-1$  is drawn as illustration. The behavior of the strongly adsorbed grafted polymers in the mean-field model therefore exhibits mean-field critical behavior in the limit of high adsorption energies.

We now need to examine two limits to verify that the adsorption-desorption transition does not reach its critical temperature: the limit for finite chain length and infinite adsorption energy and that of finite adsorption energy and infinite chain length. In Figure 11 the maximum of  $\xi$  for  $N = 50$  is logarithmically plotted as a function of  $\chi_{\text{sur}}$ . It is found that at high adsorption energies  $\xi$  scales as  $\xi_{\text{max}} \sim (-\chi_{\text{sur}})^\nu$  where  $\nu$  is approximately 5. Therefore, for a finite chain length in the mean-field model a true divergence of the segmental conformational susceptibility is only found at infinite adsorption energy, or zero temperature. The pancake-brush transition for finite chain lengths is continuous for all adsorption energies.

The behavior of the segmental conformational susceptibility as a function of the density is examined for various values of  $N$  at constant  $\chi_{\text{sur}} (-3)$  in Figure 12. Three chain lengths are used,  $N = 500, 1000$ , and  $1500$ . It is found that the change of the segmental chemical potential during the pancake-brush transition for a

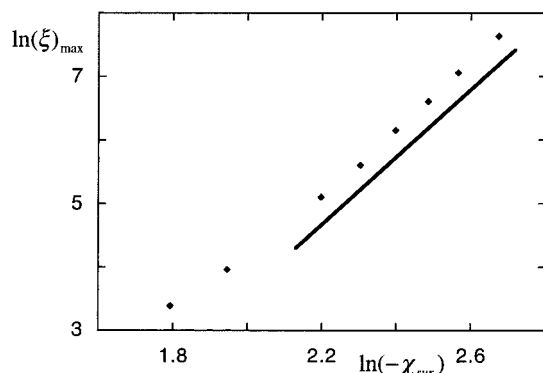


**Figure 11.** The maximum of the segmental configurational susceptibility,  $\xi$ , in the proximity of the critical density  $\theta = 1$  for various adsorption energies on a logarithmic scale. The scaling exponent of the line drawn is 5.

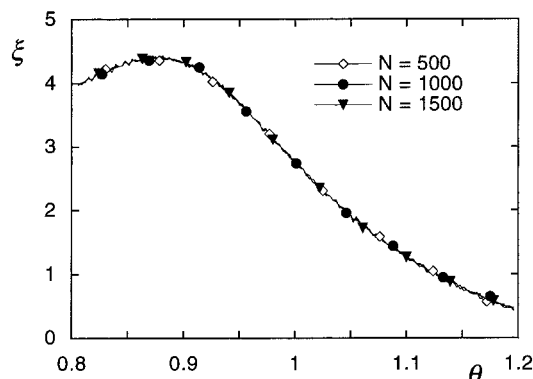


**Figure 12.** Segmental conformational susceptibility,  $\xi$ , as a function of the density  $\theta$  for  $N = 500$  (diamonds), 1000 (circles), and 1500 (triangles) with  $\chi_{\text{sur}} = -3$ .

finite adsorption energy is independent of the chain length. This agrees with the desorption process being dominated by the tail end of the grafted polymers. The entropic gain by desorption of a segment at high surface affinity and increasing surface density is independent of the total chain length, and therefore the chain length plays no significant role in this transition.

## 5. Conclusions

In this paper we have examined grafted polymer chains with surface affinity in a good solvent from two different viewpoints. In section 3 it is shown that there is a semiquantitative agreement between the Scheutjens–Fleer SCF model and experimental results for the surface pressure of grafted chains with surface affinity. The shape of the numerical isotherms agrees with that of the experimental isotherms of PS–PEO block copolymers. It is concluded that the pancake–brush transition is reproduced in a correct manner in the numerical calculations. The experimental adsorption–desorption transition of the grafted chains is characterized by a semiplateau in the surface pressure isotherm. This plateau is reproduced with the SCF model, using the same values for the chain length and segmental adsorption energy as in the experiments.

It is also found that both the experimental results for PS–PEO and the numerical data for the surface pressure as a function of the grafting density obey the SCF scaling relationships for brushes. To obtain this scaling, it is important to correct for adsorption contributions

of the grafted polymers to the surface pressure. The scaling of the asymptotic brush regime is found experimentally only for long chains. The surface pressure isotherms can be used to identify the brush regimes. Using this, the scaling of the height of long PEO chains at high grafting densities is found to agree nicely with that of the SCF scaling law. For short chains the results for the brush height do not follow this scaling law.

In section 4 the nature of the pancake–brush transition is investigated with the SCF model. It is concluded that the transition is continuous for all chain lengths and adsorption energies. This does not agree with the model of Liguore<sup>34</sup> which predicted a first-order transition in the adsorption–desorption process. It does agree qualitatively with the more recent findings of Aubouy et al. who also conclude that the transition is continuous.<sup>35</sup> The mechanism proposed in their paper, a gradual decrease in the loop distribution and subsequent formation of a quasi-brush from a self-similar adsorbed layer, does not agree with our results. We find that the pancake–brush transition is characterized as a transition from an adsorbed monolayer at low grafting densities toward desorbed tail ends at higher densities; the role of loops in the transition mechanism can be neglected.

With increasing surface affinity the system approaches a critical point with a corresponding critical behavior of the thermodynamic parameters. The critical exponent for the conformational susceptibility corresponds to that of the magnetic susceptibility of a ferromagnet in a mean-field model. The critical point itself is only reached at infinite adsorption energy. The chain length plays no significant part in the adsorption–desorption transition close to the critical point.

**Acknowledgment.** We are greatly indebted to Henri Bijsterbosch for providing the experimental data used in this paper.

## Appendix: Surface Pressure in SCF Theories for Grafted Polymers at Interfaces

Within the lattice-based SCF theory of Scheutjens and Fleer (SF–SCF) it is possible to write the canonical partition function, and thus the free energy, in terms of the optimized set of conformations of the molecules or equivalently, and more conveniently, in terms of the equilibrium density and potential profiles (see, e.g., Evers et al., referred to as ESF).<sup>41</sup> We argue that when there are grafted chains in the system, there is no closed expression for the surface pressure (a nondifferential equation in terms of segment density and potential profiles). Carignano and Szleifer (CS–SCF) (see refs 8 and 9, referred to as CSI and CSII, respectively), however, claim to have such a closed formula. The purpose of this appendix is to give more details on this issue. To rule out possible differences on fundamental grounds, we start by proving the equivalence of the free energy functionals used in the SF–SCF and the CS–SCF approach. This is done by expressing the ESF free energy in the notation used in CSI. We then point to the problems of obtaining a closed expression for the surface pressure.

In ESF a general expression for the dimensionless free energy per unit area is given

$$F = \sum_i \sigma_i \ln \frac{\sigma_i}{q_i} - \sum_z \left[ \sum_{A'} \rho_{A'}(z) u_{A'}(z) - \frac{1}{2} \sum_A \sum_B \rho_A(z) \chi_{AB} \rho_B(z) \right] \quad (\text{A1})$$

Here,  $i$  is the index which refers to the molecule types and  $z$  the index to the layer numbers which run from  $z = 1$  near the surface to  $z = M$  (far away from the surface). The summation over  $A'$  is over all segment types except the surface component; the other two summations run over all segment types in the system, including the surface component. Here, we have chosen to denote the segment densities by  $\rho$ , consistent with the notation in this paper.<sup>47</sup> Conjugated to the segment densities are segment potential profiles denoted by  $u(z)$ . In eq A1  $\sigma_i$  refers to the number of molecules  $i$  per unit area and  $q_i$  is the corresponding single-chain partition function, which is the weighted sum over all possible conformations of molecule  $i$  in the system. Finally, the contact energies are accounted for by the Flory-Huggins interaction parameters  $\chi_{AB}$ .

We can reduce eq A1 for the two-component case, where component  $i = 1$  is an end-grafted polymer of length  $N$ , and molecule  $i = 2$  is the monomeric solvent with bulk density  $\rho_0^b = 1$ . The constraint  $\rho_p(z) + \rho_0(z) = 1$  is used to write  $F$  completely in terms of the quantities of the grafted chains and the Lagrange field  $\pi_0(z)$  (see eqs 1 and 2 above where  $u'(z)$  is used for the Lagrange field):

$$F = \sigma \ln \sigma - \sigma \ln q - \sum_z [\pi_0(z) - \rho_p(z) \chi_{p0} \langle \rho_p(z) \rangle] \quad (\text{A2})$$

Here and below, we omit the label  $i=1$  for the polymer quantities. In eq A2 (fully in line with ESF: eq 1.52) we have omitted the irrelevant term  $\sigma N \chi_{p0}$ . It is easily seen that eq A2 is consistent with CSI: eq 13. The exact correspondence is obvious when realizing that there is a sign difference between the  $\chi_{p0}$  parameter in ESF and the  $\chi(|z-z'|)$  function in CSI. In addition, the angular brackets in eq A2 have exactly the same effect as the integration over  $z'$  in the  $\chi(|z-z'|)$  function of CSI. The short-range energetic interactions are irrelevant for the problem at hand and we can, in the following, discuss the athermal case ( $\chi_{p0} = 0$ ) without losing the point.

Defining  $n$  as the number of polymers in the system and  $A_s$  as the surface area in the system, we may find the surface pressure from the function  $F$  by (cf. eq 11)

$$\Pi = \sigma \left( \frac{\partial F}{\partial \sigma} \right)_{A_s} - F = - \left( \frac{\partial F A_s}{\partial A_s} \right)_n \quad (\text{A3})$$

where the quotient within the first brackets equals the chemical potential of the grafted chains. We note again that  $F$  is a dimensionless free energy per unit area and that  $\Pi$  is made dimensionless as well. As all quantities are normalized per unit area, the differentiation to the surface area is not operational. Consequently, it is needed to follow the route to differentiate  $F$  with respect to the grafting density (cf. eq A3). The problem with an analytical differentiation of  $F$  with respect to the grafting density is that both the single-chain partition function  $q$  and the Lagrange field are a function of the grafting density. Thus, the chemical potential of the grafted chains can only be found by "measuring" the

change in  $F$  when  $\sigma$  is changed slightly. We have checked that if we do this operation numerically, we find in the limit of very low surface coverages that the surface pressure approaches the ideal gas law (see Figure 1). Moreover, we checked that Gibbs's law, which can be written in the case of grafted polymers as  $\partial \Pi / \partial \mu = \sigma$ , is obeyed rigorously.

In CSII the  $\sigma \ln \sigma$  term of eq A2 was dropped by arguing that this term is only necessary when there is no grafting. We believe that this is not allowed; the effect is that in CSII the ideal gas limit for the surface pressure is not recovered. Following the SC argumentation, however, the free energy is given by  $F = -\sigma \ln q - \int_z \pi_0(z) dz$ . Inserting this in eq A3 we find for the surface pressure

$$\begin{aligned} \Pi &= \sigma \frac{\partial F}{\partial \sigma} - F = \sigma \left[ -\ln q - \sigma \frac{\partial \ln q}{\partial \sigma} - \frac{\partial \int_z \pi_0(z) dz}{\partial \sigma} \right] + \\ &\quad \sigma \ln q + \int_z \pi_0(z) dz \\ &= -\sigma^2 \frac{\partial \ln q}{\partial \sigma} - \sigma \frac{\partial \int_z \pi_0(z) dz}{\partial \sigma} + \int_z \pi_0(z) dz \\ &= \sigma^2 \int_z \rho_p(z) \frac{\partial \pi_0(z)}{\partial \sigma} dz - \sigma \frac{\partial \int_z \pi_0(z) dz}{\partial \sigma} + \int_z \pi_0(z) dz \quad (\text{A4}) \end{aligned}$$

where we have used a generic property of SCF theories that  $\partial \ln q = \int_z \rho_p(z) \partial u_p(z) dz$  and the fact that in the absence of short-range interactions  $\partial u_p(z) = \partial \pi_0(z)$ . When subsequently  $\sigma^2$  is **wrongly** replaced by  $\sigma$ , the CSII (eq 7) result is found in just a few steps:

$$\Pi = \int_0^\infty \pi_0(z) dz - \sigma N \propto (\sigma N)^2 + O(\sigma^3) \quad (\text{A5})$$

On the right-hand-side (rhs) of eq A5 we have used the fact that the Lagrange field can be approximated by

$$\begin{aligned} \pi_0(z) &= -\ln \frac{\rho_0(z)}{\rho_0^b} = -\ln \frac{1 - \rho_p(z)}{1 - \rho_p^b} \approx (\rho_p(z) - \rho_p^b) + \\ &\quad \frac{1}{2}(\rho_p(z) - \rho_p^b)^2 + O()^3 \quad (\text{A6}) \end{aligned}$$

Here,  $\rho_p^b$  is the density of polymer in the bulk which is, in the case of grafting, identical to zero. Clearly, the result of eq A5 does not comply with the ideal gas law for low surface coverages, as also mentioned in CSII. We note again that the ideal gas contribution can be inserted in eq A5 if in the free energy equation the term  $\sigma \ln \sigma$  is kept.

It is instructive to consider the case that all molecules in the system can equilibrate with the bulk. This case has been worked out in ESF and starts obviously at eq A1. The surface pressure for a two-component polymer-solvent system can be written in the form (ignoring again the energetic terms for simplicity)

$$\begin{aligned} \Pi &= - \left( 1 - \frac{1}{N} \right) (\sigma N - M \rho_p^b) + \sum_{z=1}^M \pi_0(z) \approx \\ &\quad \sigma - \frac{M \rho_p^b}{N} \approx \sigma^{\text{exc}} \quad (\text{A7}) \end{aligned}$$



where  $\sigma^{\text{exc}}$  is the excess number of polymer molecules per unit area at the surface. The result of eq A7 is the ideal gas law for the surface pressure in dimensionless form (found at low adsorbed amounts). From the above it is clear that it is misleading to think that the Lagrange field profile and the surface pressure are directly linked. In fact, from eq A7 we find that the Lagrange field contribution cancels out in first approximation at low excess adsorbed amounts.

It is tempting to apply eq A7 to the case where the polymers are grafted by substituting  $\rho_p^b = 0$  in eq A7. Interestingly, eq A4 is recovered (including the dropped term). In equilibrium, however, there is a one-to-one relation between the excess number of polymers at the surface and the chemical potential of the polymers, and thus with the polymer bulk concentration  $\rho_p^b$ . By setting  $\rho_p^b = 0$ , one needs to put  $\sigma = 0$  as well, even when there is a very strong anchor group binding the polymer with one end to the surface. Indeed, for a fixed  $\sigma$ , the bulk density of the polymer can practically approach zero when the grafting energy is increased correspondingly. But for a fixed surface affinity of the anchor group (no matter how high this is), it is always possible to lower the bulk concentration in order to reduce the amount of adsorbed polymers. Thus, the mathematical point of no polymers in the bulk,  $\rho_p^b = 0$ , is only compatible with no polymers at the interface, that is,  $\sigma = 0$ . Again, we find that eq A5 is not the correct expression for the surface pressure in a system where polymers are grafted to an interface.

We thus conclude that eq A4 is wrong. The error in the derivation of CS has been identified and a complementary route to obtain eq A5 was shown to be wrong as well. Therefore, the only way to obtain the surface pressure in a system that features grafted chains is by numerical differentiation.

## References and Notes

- Halperin, A.; Tirrell, M.; Lodge, T. P. *Adv. Polym. Sci.* **1992**, *100*, 31.
- Misra, S.; Varanasi, S. *J. Colloid Interface Sci.* **1991**, *146*, 251.
- Kuhl, T. L.; Leckband, D. E.; Lasic, D. D.; Israelachvili, J. N. *Biophys. J.* **1994**, *66*, 1479.
- Lasic, D. D.; Martin, F. J.; Gabizon, A.; Huang, S. K.; Papahadjopoulos, D. *Biochim. Biophys. Acta* **1991**, *1070*, 187.
- Alexander, S. *J. Phys. (Paris)* **1977**, *38*, 983.
- de Gennes, P.-G. *Macromolecules* **1980**, *13*, 1069.
- Wijmans, C. M.; Scheutjens, J. M. H. M.; Zhulina, E. B. *Macromolecules* **1992**, *25*, 2657.
- Carignano, M. A.; Szeifler, I. *J. Chem. Phys.* **1994**, *100*, 3210.
- Carignano, M. A.; Szeifler, I. *Macromolecules* **1995**, *28*, 3197.
- Martin, J. I.; Wang, Z. G. *J. Phys. Chem.* **1995**, *99*, 2833.
- Lai, P. Y.; Binder, K. *J. Chem. Phys.* **1992**, *97*, 586.
- Grest, G. S. *Macromolecules* **1994**, *27*, 418.
- Subramanian, G.; Williams, D. R. M.; Pincus, P. A. *Macromolecules* **1996**, *29*, 4045.
- Yeung, C.; Balazs, A. C.; Jasnow, D. *Macromolecules* **1993**, *26*, 1914.
- Wagner, M.; Brochard-Wyart, F.; Hervet, H.; de Gennes, P.-G. *Colloid Polym. Sci.* **1993**, *271*, 621.
- Tang, H.; Szeifler, I. *Europhys. Lett.* **1994**, *28*, 19.
- Zhulina, E. B.; Borisov, O. V.; Priamitsyn, V. A.; Birshtein, T. M. *Macromolecules* **1991**, *24*, 140.
- Semenov, A. N. *Sov. Phys. JETP* **1985**, *61*, 733.
- Milner, S. T.; Witten, T. A.; Cates, M. *Macromolecules* **1988**, *21*, 2610.
- Skvortsov, A. M.; Pavlushkov, I. V.; Gorbunov, A. A.; Zhulina, E. B.; Borisov, O. V.; Priamitsyn, V. A. *Polym. Sci. U.S.S.R.* **1988**, *30*, 1706.
- Patel, S.; Tirrell, M. *Colloids Surf.* **1988**, *31*, 157.
- Ansarifar, M. A.; Luckham, P. F. *Polymer* **1988**, *29*, 329.
- Marra, J.; Hair, M. L. *Colloids Surf.* **1988**, *34*, 215.
- Whitmore, M. D.; Noolandi, J. *Macromolecules* **1990**, *23*, 3321.
- Field, J. B.; Toprakcioglu, C.; Ball, R. C.; Stanley, H. B.; Dai, L.; Barford, W.; Penfold, J.; Smith, G.; Hamilton, W. *Macromolecules* **1992**, *25*, 434.
- Baranowski, R.; Whitmore, M. D. *J. Chem. Phys.* **1995**, *103*, 2343.
- Bijsterbosch, H. D.; de Haan, V. O.; de Graaf, A. W.; Leermakers, F. A. M.; Cohen Stuart, M. A.; van Well, A. A. *Langmuir* **1995**, *11*, 4467.
- Factor, B. J.; Lee, L. T.; Kent, M. S.; Rondelez, F. *Phys. Rev. E* **1993**, *48*, 2354.
- Kent, M. S.; Lee, L. T.; Farnoux, B.; Rondelz, F. *Macromolecules* **1992**, *25*, 6240.
- Kent, M. S.; Lee, L. T.; Factor, B. J.; Rondelez, F.; Smith, G. H. *J. Chem. Phys.* **1995**, *103*, 2320.
- Auroy, P.; Auvray, L.; Léger, L. *Phys. Rev. Lett.* **1991**, *66*, 719.
- Auroy, P.; Auvray, L.; Léger, L. *Macromolecules* **1991**, *24*, 2523.
- Richards, R. W.; Rochford, B. R.; Webster, J. R. P. *Polymer* **1997**, *38*, 1169.
- Ligoure, C. *J. Phys. II (Paris)* **1993**, *3*, 1607.
- Aubouy, M.; Guiselin, O.; Raphaël, E. *Macromolecules* **1996**, *29*, 7261.
- Ou-Yang, D.; Gao, Z. *J. Phys. II (Paris)* **1991**, *1*, 1375.
- Cao, B. H.; Kim, M. W. *Faraday Discuss.* **1994**, *98*, 245.
- Scheutjens, J. M. H. M.; Fleer, G. J. *J. Phys. Chem.* **1979**, *83*, 1619.
- Scheutjens, J. M. H. M.; Fleer, G. J. *J. Phys. Chem.* **1980**, *84*, 178.
- Silberberg, A. *J. Chem. Phys.* **1968**, *48*, 2835.
- Evers, O. A.; Scheutjens, J. M. H. M.; Fleer, G. J. *Macromolecules* **1990**, *23*, 5221.
- Brandrup, J.; Immergut, E. H. *Polymer Handbook*, 3rd ed.; Wiley: New York, 1989.
- Zhulina, E. B.; Borisov, O. V.; Priamitsyn, V. A. *J. Colloid Interface Sci.* **1990**, *137*, 495.
- Molyneux, P. *Water-soluble synthetic polymers: properties and behaviour*; CRC Press: New York, 1983.
- Cardy, J. *Scaling and Renormalization in Statistical Physics*; Cambridge University Press: Cambridge, 1996.
- Davis, T. D. *Statistical Mechanics of Phases, Interfaces and Thin Films*; VCH: New York, 1996.
- In ESF the notation  $\varphi$  is implemented whereas in CS's work the notation  $\langle\varphi(z)\rangle$  is used for these quantities. In the SF-SCF theory the angular brackets have the function to account for the nonlocal contacts and therefore we choose here to use  $\rho$  instead.

MA970525K